

# Limitations on Energy Deposition in Solid and Liquid Targets and Jet Liquid Target Description.

G.I. Silvestrov and T.A. Vsevolozhskaya

Institute for Nuclear Physics  
Novosibirsk, USSR

Target problems are among the important as in the current runs of TEVATRON collider so in the most degree in its upgrades [1]. Focusing of  $5 \cdot 10^{12}$  protons onto a target in a spot of  $\approx 0.15$  mm size will provide the deposited energy density of 1.5 kJ/gr in a copper target and of 3.2 kJ/gr in that of tungsten. To present time sufficient experimental data are stored in FNAL so as in CERN concerning to target material destruction caused by intensive proton beam. Let us try to understand the nature and features of such a destruction considering the material behaviour from the hydrodynamical point of view which represents the most common laws of material transformation, that of mass, energy and momentum conservation, and is quite admissible if values of preassure exceed the fluidity limit.

Energy deposition in target material leads to a rise of preassure in the region where such a deposition takes place, thus inciting a compressive wave propagation into the outer space. Simultaneously the decompressive wave propagates into the region of energy deposition from its boundary to the center. The preassure in decompressive wave can fall below zero and if this negative preassure exceeds the limit of material stability for expansion, the destruction occurs. The stability limit is determined by the Brinell hardness  $H_B$  of material [2].

In the acoustic approach to the hydrodynamical consideration with the equation of state in simple empiric form

$$E = E_c + E_T$$

$$P = - \frac{dE_c}{dV} + \frac{\Gamma E_T}{V},$$

where  $E$  is the specific value of internal energy,  $E_c = \frac{C_0^2}{2} \left(1 - \frac{V_0}{V}\right)^2$  and  $E_T$  - its potential and thermal components,  $V$  - specific volume of material,  $\Gamma$  - Gruneisen coefficient,  $C_0$  - sound speed, the value of preassure  $P$  at the beam axis not too close to inlet or outlet target surfaces is determined as:

$$P = \frac{\Gamma Q_0}{C_0 V_0 \tau} \left\{ \int_0^{C_0 t} e^{-\frac{C_0^2 t^2 - x^2}{2 \delta^2}} dx - \int_0^{\max\{0, C_0(t-\tau)\}} \exp\left\{-\frac{C_0^2(t-\tau)^2 - x^2}{2 \delta^2}\right\} dx \right\} (1)$$

where  $Q_0$  stands for specific value of deposited energy at the center of its trasverse distribution which is considered gaussian with r.m.s. width  $\delta$ , while the longitudinal distribution of energy and time structure of particle beam are considered homogeneous. Duration of beam spill onto the target is denoted by  $\tau$ . Expression for  $E$  is empiric one taken from [3].

At a fixed value of  $Q$  the preassure depends significantly on  $\tau$ . It is maximum, if  $\tau$  is much shorter than a time  $t_k$  of sound propagation across the region where the energy deposition takes place. Its value then is  $P = \Gamma Q/V_0$  and decompressive preassure achieves the value of  $(-P)_{\max} = 0.285 \Gamma Q_0/V_0$ .

If spill duration is large as compared to  $t$  the values of preassure are about  $t_k/\tau$  times less, than in the case where  $\tau \ll t_k$ . The maximum decompressive preassure at the beam axis is

$$(-P)_{\max} \approx \frac{\Gamma Q_0}{V_0} \cdot \frac{\epsilon}{1.19(C_0 \tau + 1.19\epsilon)} \quad (2)$$

If beam consists of a series of bunches with intervals much shorter than  $t_k$ , its time structure could be considered as homogeneous.

At fig.1 the decompressive preassure in tungsten target for the proton beam parameters such as in the corresponding run (r.m.s. beam spot size  $\epsilon = 0.28$  mm) is shown versus  $Q_0$  in comparison with the hardness  $H$  dependence on temperature. The value of  $\epsilon$  for energy density distribution is taken equal to  $\epsilon = 0.7$  mm that fits the calculated data [4], spill duration is 1.67 mcs. Two curves of  $H_g$  per temperature represent two kinds of tungsten - a hard and an annealed ones. In both cases the intersection with line  $(-P)_{\max}$  versus  $Q_0$ , that determines the limit value of energy density, takes place near  $Q_0 = 200$  J/gr in an excellent harmony with experimental data. Another conclusion from the above consideration - the localization of material damage within the region of energy deposition, where high temperature and negative preassure take place simultaneously, also well agrees with experimental evidence.

In the case of copper target the hardness value and its reduction with temperature are strongly dependent on type of copper. At fig.2 the  $H$  versus temperature is shown for one of them - C92260. Here the hardness falling down with temperature rise up to about  $100^\circ\text{C}$ , keeps almost constant value of  $H_g = 57$  kg/mm<sup>2</sup> at higher temperatures, thus predicting the limit value of  $Q_0$  being of the order of 460 J/gr for energy distribution width  $\epsilon = 0.6$  mm which comes from [4] for beam width of a current run  $\epsilon = 0.18 - 0.20$  mm. It is not in bad accord with the value  $Q_0 = 420 - 370$  J/gr following out of [4] for current run with  $2 \cdot 10^{12}$  protons per spill.

Mechanical limit for energy deposition density in copper target looks to be able to increase if a proper type of copper would be chosen among the multitude of them, some having the twice or so higher value of  $H$  than used in above evaluation, however it would hardly permit to exceed the melting energy - the sum of energy for heating up to the melting point and the latent melting energy - equal to about 680 J/gr.

In the liquid target the main limiting factor is the so called mass depletion effect, i.e. the significant decrease in target density during beam spill in the region of beam travel. From that point of view the severe limitation arises to a choice of target material. Nor mercury looking so proper nor lead could be taken because of early start of mass

depletion. The energy density per proton in lead is close to that in tungsten, i.e. it is to be of the order of 2 kJ/gr already after the phase I of accelerator upgrade fulfillment. By that the material density at the beam axis will decrease to the end of beam spill in more than five times from its initial value. As to the mercury where the energy density would be of the same order, it should be evaporated during the first quarter of beam spill. So the only materials which meet the targeting conditions are that with high energy of sublimation and low enough melting point. The gold and the copper seem to meet both these requirements.

In copper the density  $\rho$  dependence on specific value of energy deposition at the beam axis is well described by the expression (3) [5]

$$\rho = \rho_0 e^{-\Gamma Q_0 / C^2} \quad (3)$$

With  $Q_0$  equal to 1.5 kJ/gr density reduction to the end of beam spill will be equal to 18% that means about 10% loss in the medium density.

Crucial value of  $Q$  may occur to be that corresponding to store of about a half of the latent energy of vaporization. Near this point the value of  $d^2 E_c / dV^2$ , where  $E_c(V)$  is internal potential energy of material, changes its sign that means the attractive forces in material begin to weaken with an increase of specific volume. It may result in an instability of liquid metal jet under the beam exposure.

If gold is considered as a material for liquid target the specific energy per proton should be about the same as in tungsten, i.e. two times more than in copper and accordingly more will be the mass depletion effect. Moreover, the energy for vaporization, including heating from melting to boiling point and the latent energy of vaporization, is about 2.1 kJ/gr only and 3 kJ/gr energy deposition will be much above admissible.

So the heavy metals, having high density of energy deposition, looks to be of no good as concerning the mass depletion effect. They are nevertheless of much use for the cases where not the deposited density of energy per spill but that of medium power is high, so as it occurs in the electron - positron conversion systems operating at high repetition rate.

Development of jet liquid targets is now in progress in the Institute for Nuclear Physics in Novosibirsk [6]. The technology is practically worked out for target of Ga-In alloy, whose melting temperature is 18°C only. Such a target made as a flat jet of liquid metal flowing with a stationary velocity of several meters per second was already produced and sent to IHEP in Protvino for tests under the proton beam. The scheme of target device is shown in fig.3. It consists of vacuum chamber with electromagnetic pump and drain cavity with a nozzle of 25 cm length which the metal jet is draining through. Jet thickness could be changed from one to several millimeters by changing the width of nozzle. Full volume of liquid metal in system is equal to 500 cubic cm. The system could be heated up to several hundreds degree thus allowing to try the materials with higher melting temperature. The conditions for optimum

operation efficiency of Ga-In system were studied and test run during 500 hours was worked out before the system was sent to IHEP. These conditions include the filling of the system with an inert gas of the purity of 10 - 100 ppm under a preassure of about 1 atmosphere. At present the system is under a preparation for the test with proton beam.

The same design scheme was adopted for the development of system for high ,more than 500°C, operating temperature but its size is to be made as small as possible and as a material of its manufacture of is chosen the graphite. Graphite is high temperature and chemically resistive, and transparent for magnetic flux that is necessary for proper operation of our pumps. At present the technology for super strong materials production at the base of graphite fibres and fabrics is in good progress in the industry. Elaboration of technology of graphite chamber production is carried on in collaboration with Moscow institute NIIGraphite.

The scheme of target device is shown in figure 4. Its outer size is about 100\*120\*120 mm. The optimisation of geometry was fulfilled on a chamber of organic glass with liquid Ga-In alloy. That permitted to watch the way of metall flowing through the system. At present the geometry is mainly chosen and chamber of graphite is manufactured. Nozzle length is 50 mm and width is variable from 0.5 to 2 mm. The nearest plans are to test the system with liquid lead.

First version of high temperature target device will not have an aperture for beam to go in and out. Beam will pass through 5 - 10 mm thick graphite walls or through windows in it closed with titanium or berillium foils.

In its final version the target device, put into vacuum chamber with special system for gas evacuation and with inputs for pump feeding, will be placed on an adjusting mechanism with distant two coordinate replacement under the beam. The pump is fed from a special thyristor inverter operating with 2 kHz frequency.

#### References

-----

1. Fermilab Accelerator Upgrade. Phase I. April 1989  
Fermilab Upgrade Phase II: The Main Injector. April 10, 1989
2. YU.B.Zel'dovich and Yu.P.Raizer. Physics of Shock Waves and High-Temperature Hydrodynamics Phenomena. Academic Press, New York, 1967.
3. J.P.Somon. L.G.I. Rep. 64/3, 1964.
4. I.L Azhgirey and N.V.Mokhov. Antiproton Production and Energy density Limitation in Targets for the Fermilab Pbar Source. Fermilab TM-1529

5. T.A.Vsevolozhskaya. The Linear Approximation to the Hydrodynamic Consideration of Target Behaviour under High Density Beam Exposure. Preprint 84-88. Novosibirsk 1984.
6. G.I.Silvestrov. Problems of Intense Secondary Beams Production. Proc. XIII Int. Conf. on High Energy Accelerators. Novosibirsk. August 1986.

#### Figure captions

-----

- Fig.1. Hardness  $H_g$  and the maximum destructive pressure versus energy density deposition in tungsten.
- Fig.2. Hardness  $H_g$  of copper C92200 in dependence on temperature.
- Fig.3. Stationary jet target. 1 - observation window, 2 - beam axis, 3 - drain chamber, 4 - nozzle, 5 - liquid metal, 6 - pump.
- Fig.4. Jet target device of graphite. 1 - liquid metal, 2 - graphite chamber, 3 - pump, 4 - strengthened pump carcass, 5 - thermoinsulating screen, 6 - coil of electromagnet, 7 - magnet flux conductor, 8 - ceramic supports, 9 - drain chamber, 10 - magnet plug, 11 - channels for flux conductor introduction.

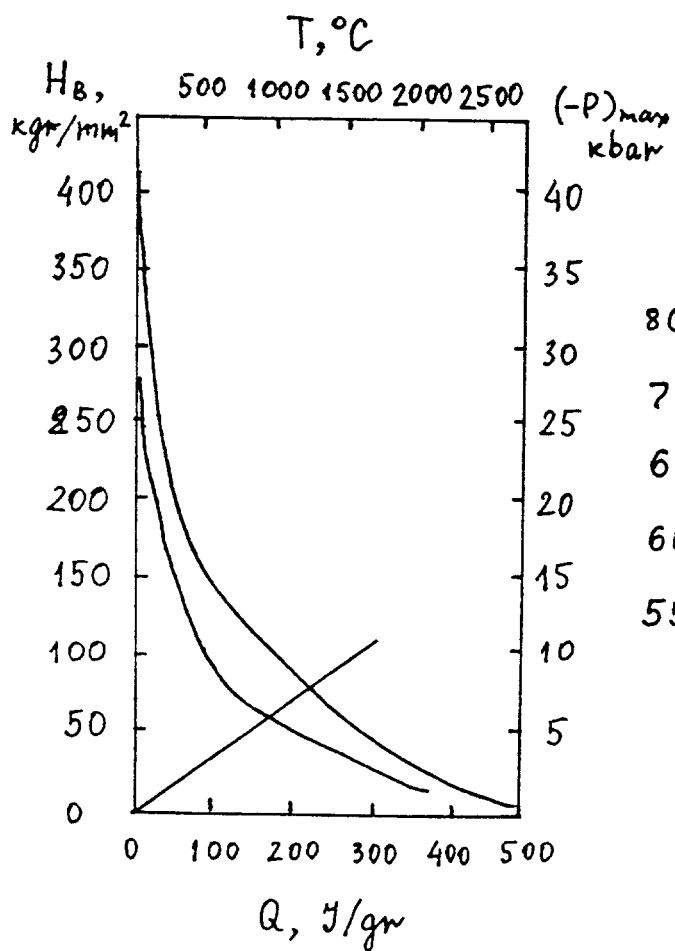


Fig. 1.

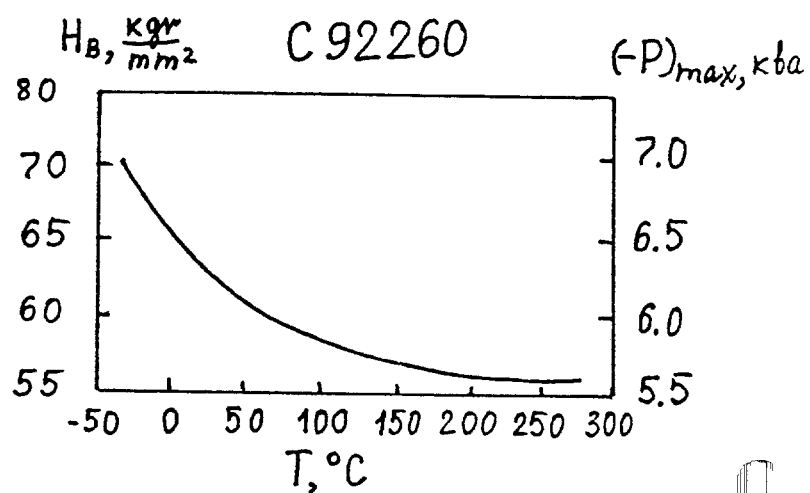


Fig. 2

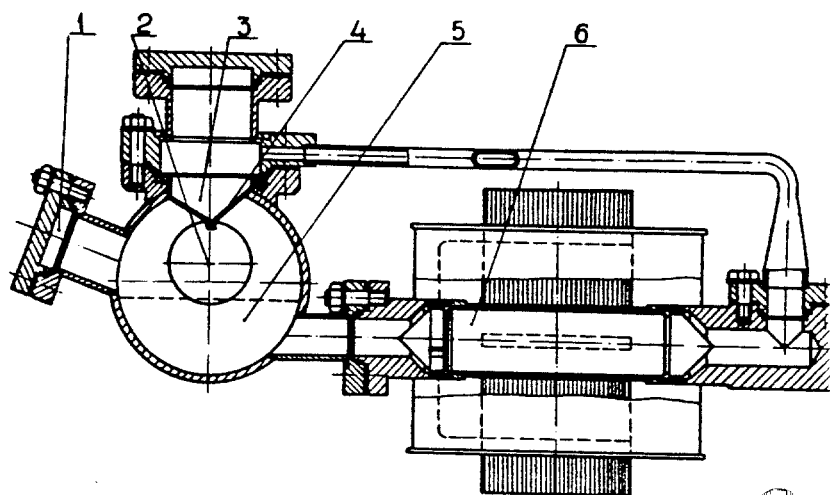


Fig. 3

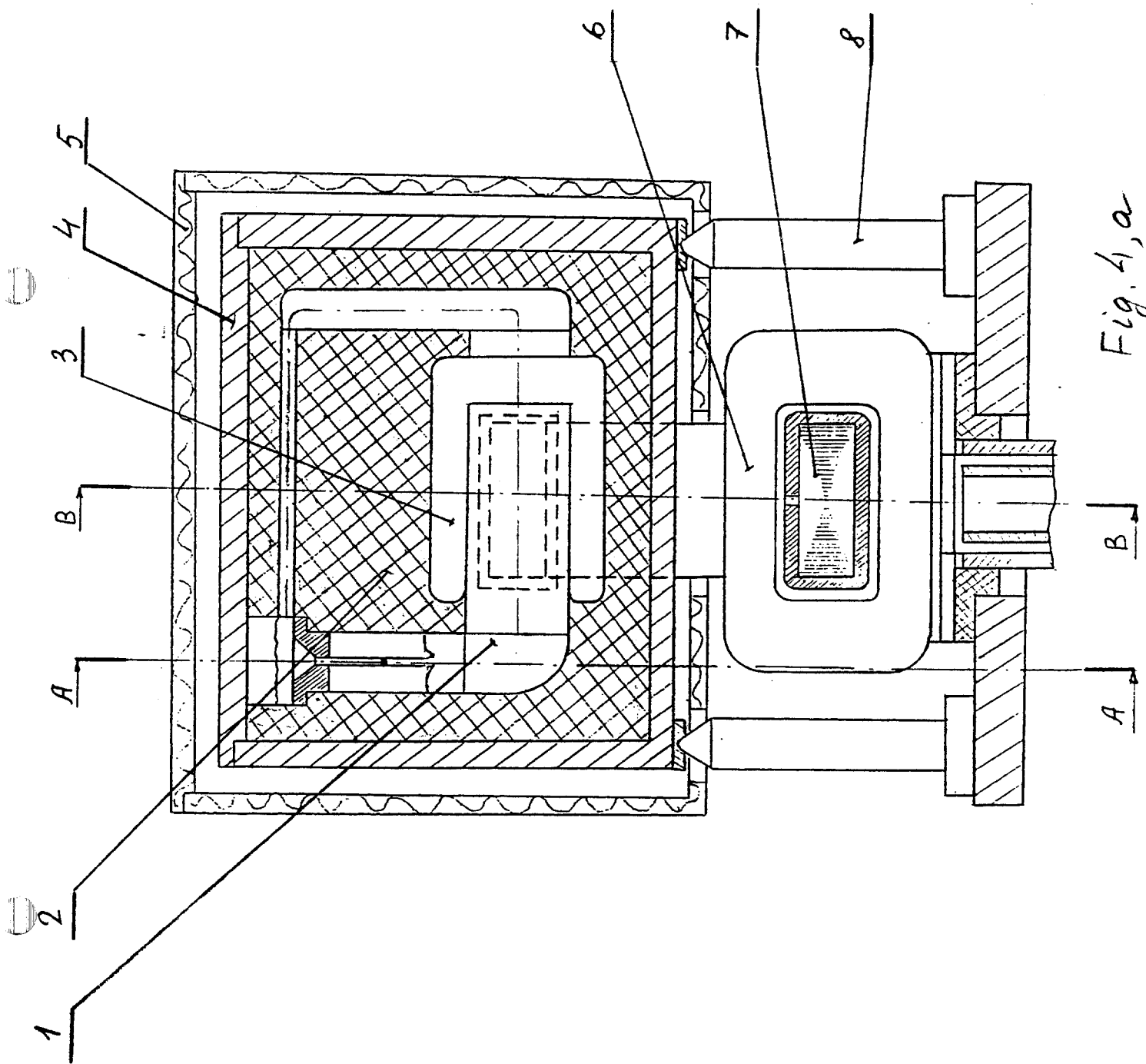


Fig. 4, a

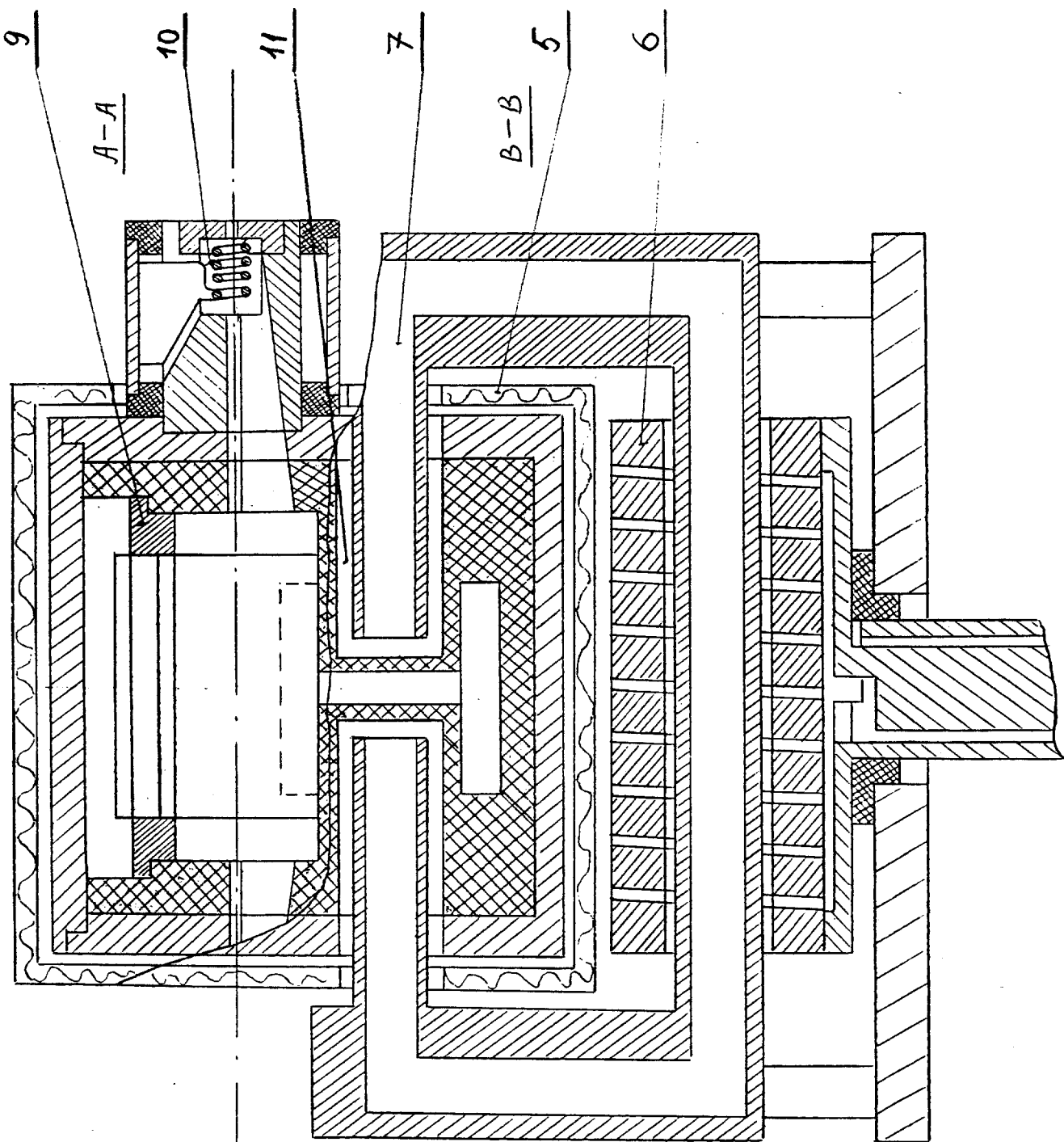


Fig. 4, b